Electronic Supplementary Material (ESI) for Physical Chemistry Chemical Physics.

Electronic Supplementary Information

Charge carrier dynamics of methylammonium lead iodide: From PbI_2-rich to low-dimensional broadly emitting perovskites

Johannes R. Klein, Oliver Flender, Mirko Scholz, Kawon Oum and Thomas Lenzer**

Universität Siegen, Physikalische Chemie, Adolf-Reichwein-Str. 2, 57076 Siegen, Germany. Email: oum@chemie.uni-siegen.de, lenzer@chemie.uni-siegen.de

Contents

S1. Changes of XRD patterns for x = 0.71 upon annealing

In Fig. S1, we present two XRD patterns of a $(MAI)_x(PbI_2)_{1-x}$ thin film with x = 0.71 during heating at 90 °C. According to the "pseudobinary phase-composition processing diagram" of Song *et al.*,[1] a mixture of stacked perovskite sheet (SPS) and low-dimensional perovskite (LDP) structures should be formed initially. Indeed, after 15 min (black line) we see perovskite XRD peaks at 14.1 and 28.4° and an LDP peak at 11.5°. Heating for 60 min (red line) leads to a decay of the LDP peak and an increase of the peak at 28.4°. The behavior is quite similar to that observed by Song *et al.* (see Fig. S3b in their Supporting Information).[1] It appears as if a thermally induced structural rearrangement or transformation of the LDP phase occurs, possibly resulting in smaller isolated 3D perovskite structures. In addition, an increased disorder of the LDPs might contribute to the reduction of the peak at 11.5°.

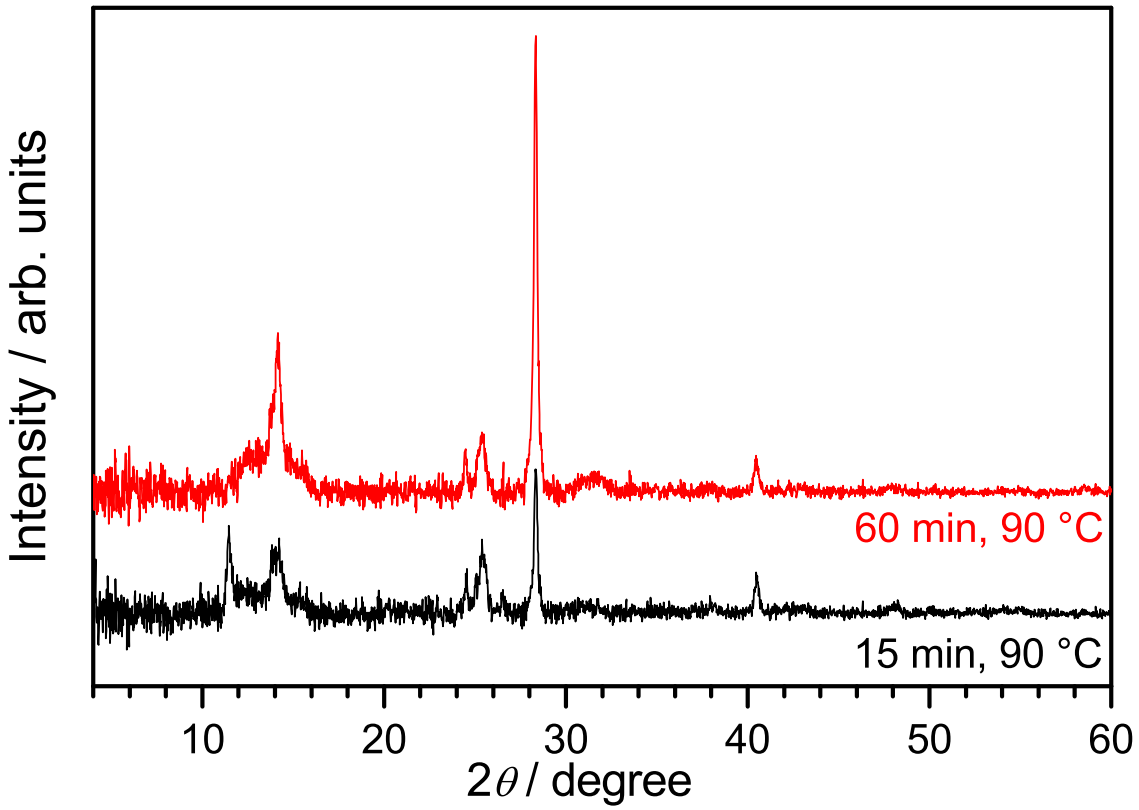

Fig. S1 XRD patterns of a $(MAI)_x(PbI_2)_{1-x}/TiO_2$/glass sample with x = 0.71. The black and red XRD patterns are obtained during annealing at 90 °C for 15 and 60 min, respectively.

S2. Optimized annealing condition monitored by XRD

The optimized annealing condition was found to be heating the $(MAI)_x(PbI_2)_{1-x}$ thin films at 90 °C for 60 min. No perovskite degradation was taking place under these conditions, as demonstrated by the black, green and red XRD patterns, taken at three different times, shown in Fig. S2 for x = 0.50. Increasing the hotplate temperature to 107 °C leads to PbI_2 formation already after 15 min, with almost complete conversion of the perovskite into PbI_2 reached after 60 min, as also shown in Fig. S2. The decomposition process was further confirmed by recording complementary transient absorption spectra of these films. After 60 min, only a weak residual absorption at 520 nm with a long tail extending into the NIR is visible, consistent with absorption features of PbI_2.[2]

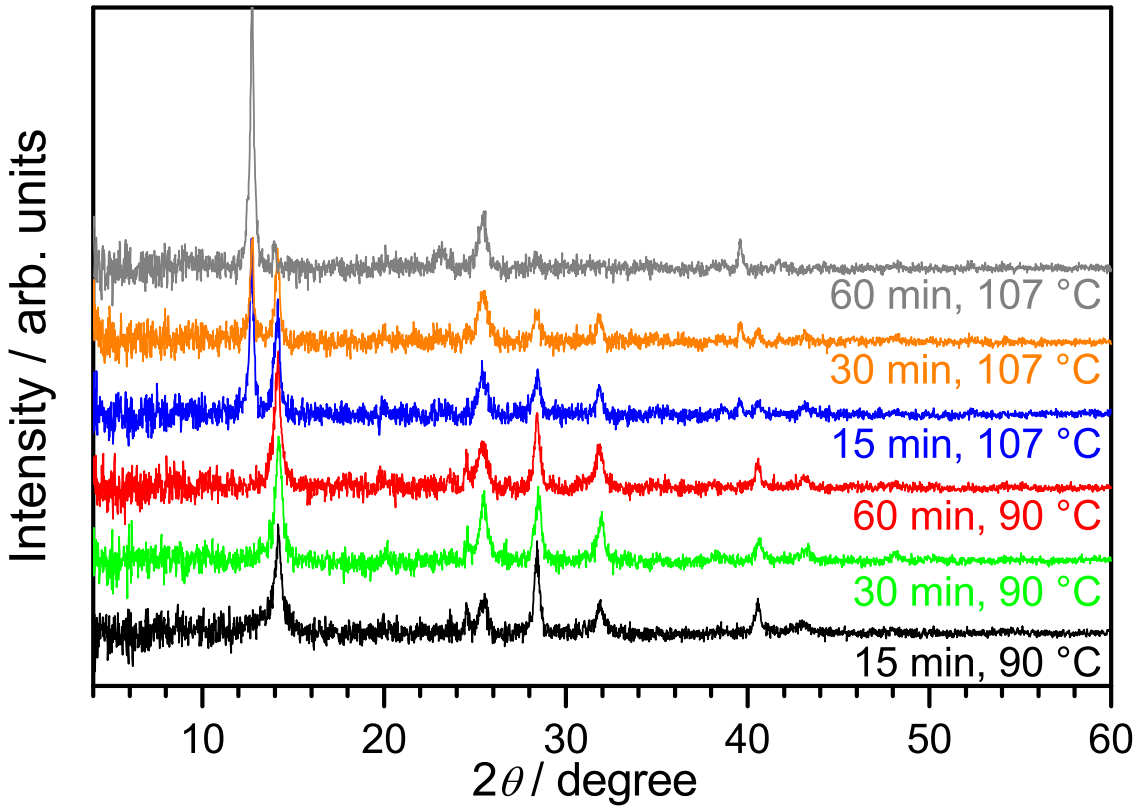

Fig. S2 XRD patterns of $(MAI)_x(PbI_2)_{1-x}/TiO_2$/glass samples with x = 0.50. The black, green and red XRD patterns are obtained during annealing at 90 °C for 15, 30 and 60 min, respectively. The blue, orange and grey XRD patterns are for annealing at 107 °C for 15, 30 and 60 min, respectively.

S3. Transient Vis-NIR spectra at the pump fluence 14 μJ cm^{-2}

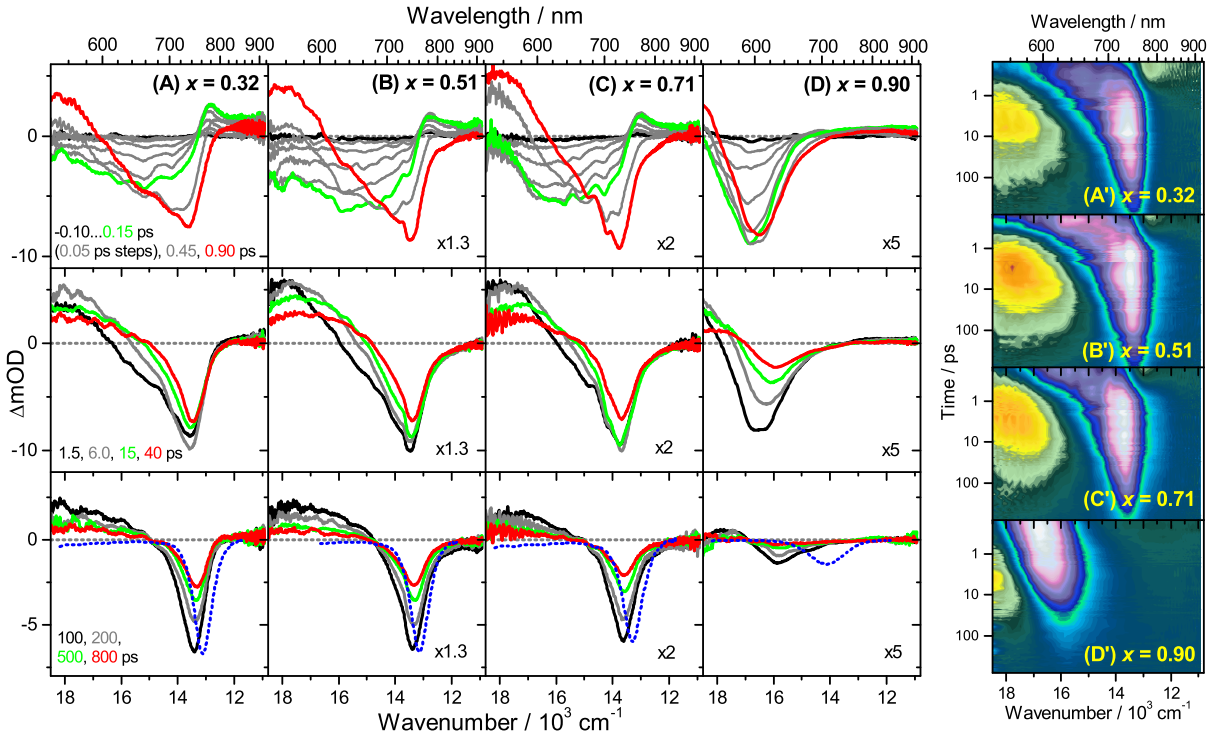

Fig. S3 Transient Vis-NIR PSCP broadband absorption spectra of $(MAI)_x(PbI_2)_{1-x}/TiO_2$/glass at a pump pulse fluence of 14 μJ cm^{-2} for different initial mole fractions *x*. Columns (A) to (D) are the results for *x* = 0.32, 0.51, 0.71 and 0.90, respectively. (Top panels) -0.10...0.15 ps with 50 fs steps; 0.45 ps, 0.90 ps; (middle panels) 1.5, 6.0, 15 and 40 ps; (bottom panels) 100, 200, 500 and 800 ps. Selected transient spectra are shown as thick colored lines for guidance. The blue- dotted lines in the bottom panels are the corresponding scaled steady-state stimulated emission spectra. (A'-D') show the dynamics of the systems in (A-D) as contour plots using a logarithmic time scale. White, pink and bluish colors denote bleach or stimulated emission, whereas green, yellow and red colors correspond to transient absorption.

S4. Analysis of recombination kinetics

As described in the main manuscript, the second-order recombination rate constant k_2 was obtained *via*:

$$\frac{1}{n(t)} - \frac{1}{n_0} = k_2 t \quad \text{with} \quad n_0 = \alpha F / E_{\text{ph}} \qquad \text{(S1)}$$

Here, n_0 and $n(t)$ are the number density of carriers in cm^{-3} at t = 0 and at a given time t, respectively, k_2 is the bimolecular rate constant in $cm^3\ s^{-1}$, α is the absorption coefficient in cm^{-1} at the pump wavelength (500 nm), F is the fluence of the pump laser beam in $\mu J\ cm^{-2}$ and E_{ph} is the pump photon energy in μJ at 500 nm.

As it turned out, the maximum ΔOD around 750 nm does not linearly depend on the fluence. A similar saturation behavior was previously found by Kamat and co-workers for two semiconductor systems.[3,4] Therefore, an empirical calibration curve for ΔOD/OD as a function of the number density of carriers $n(t)$ had to be established. This was done as follows:

The $1/\Delta OD_{t=0}$ value around 750 nm was determined at a certain pump fluence, by extrapolating the $1/\Delta OD(t)$ data for t > 10 ps to t = 0. This way, the influence of carrier cooling effects on the recombination kinetics was minimized. We normalized $\Delta OD_{t=0}$ with respect to the OD at the pump wavelength 500 nm. The normalized $\Delta OD_{t=0}$ values were then plotted as a function of F, resulting in typical saturation curves, as shown for one example (x = 0.51) in Fig. S4.

Next, the experimental $\Delta OD(t)$ values were converted into $n(t)$ with the corresponding calibration curve. Here we took $n(t)$ to be $F \cdot \alpha / E_{ph}$ in units of cm^{-3}. One result based on the data in Fig. S4 is shown in Fig. S5. The expression $y = A \cdot [\exp(B \cdot x^C)-1]$ was used for fitting the data points.

The final second-order kinetics plot was then obtained from eq. (S1). An example of such a representation is shown in Fig. S6 for x = 0.51 at different pump fluences in the range 0.7-50 $\mu J\ cm^{-2}$. All lines are largely coincident in the fluence range 2-50 $\mu J\ cm^{-2}$. At high fluence (*e.g.* > 50 $\mu J\ cm^{-2}$), there is a deviation from linearity at early times (< 100 ps). This is possibly due to some contribution of additional carrier recombination processes, which are not following simple second-order kinetics. From the global fit of the data at different fluences, we finally obtain the recombination rate constant $k_2 = (3.5 \pm 0.2) \times 10^{-9}\ cm^3\ s^{-1}$ for x = 0.51. We performed the same analysis for x = 0.32, 0.71 and 0.90. The results are shown in Fig. 8 of the main manuscript.

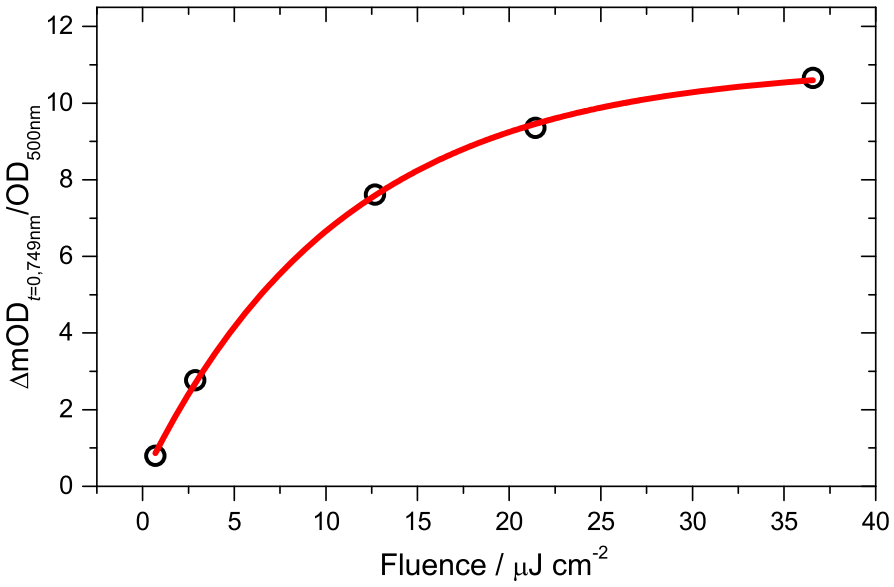

Fig. S4 Normalized $\Delta mOD_{t=0}$ values as a function of the fluence of the pump laser pulse for an $(MAI)_x(PbI_2)_{1-x}/TiO_2$/glass sample with mole fraction x = 0.51. The fluences of the pump laser beam are: F [μJ cm^{-2}] = 0.69, 2.9, 12.7, 21.4 and 36.6.

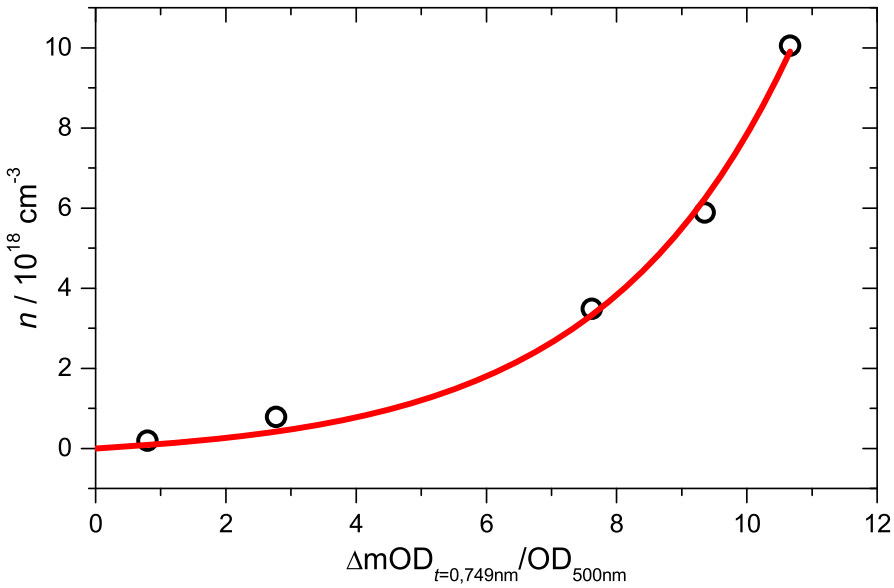

Fig. S5 An example of a calibration curve for converting experimental ΔmOD(t) into $n(t)$ values. The same experimental data as in Fig. S4 were used. Here we take n_0 to be $F \cdot \alpha$, with the fluence in units of cm^{-2}. The corresponding n_0 values are: (304 nW) 1.9 × 10^{17} cm^{-3}, (1.3 μW) 7.9 × 10^{17} cm^{-3}, (5.6 μW) 3.5 × 10^{18} cm^{-3}, (9.4 μW) 5.9 × 10^{18} cm^{-3} and (16.1 μW) 1.0 × 10^{19} cm^{-3}. The red solid line is the fit result.

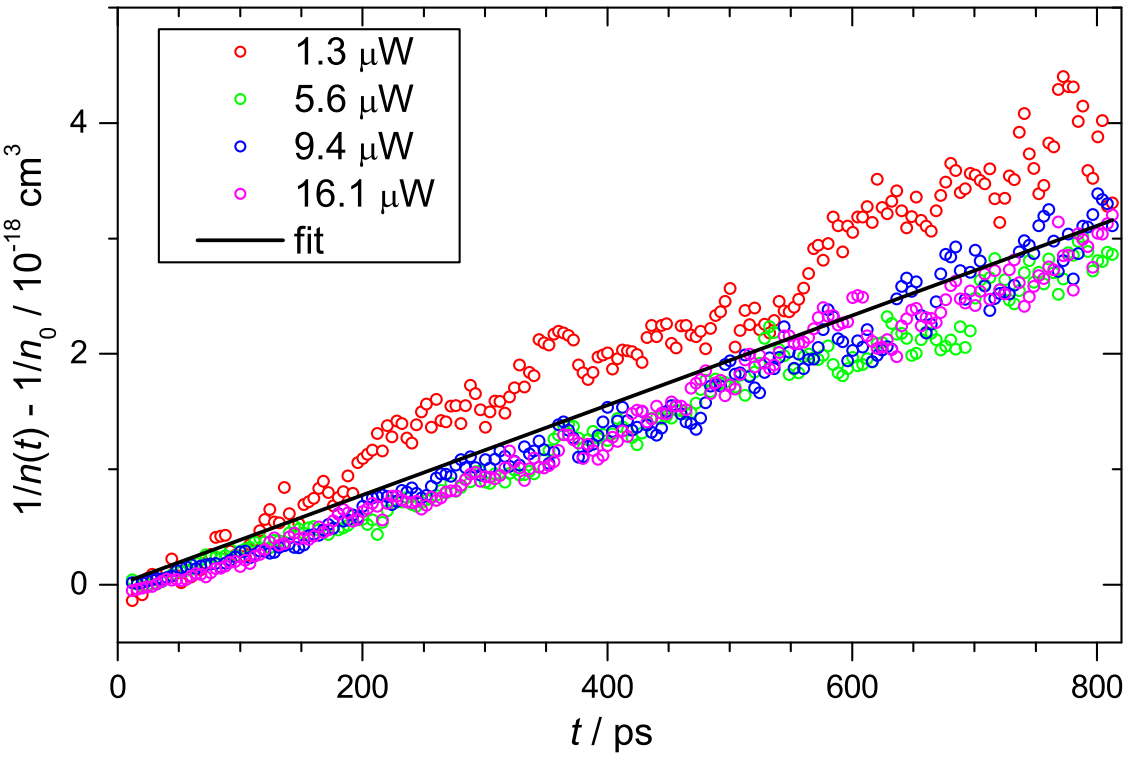

Fig. S6 Plot of the difference of the reciprocal transient (n) and initial (n_0) carrier density as a function of time for an $(MAI)_x(PbI_2)_{1-x}/TiO_2$/glass sample employing the mole fraction x = 0.51. The black line represents the global fit to all data points.

References

1. Z. Song, S. C. Watthage, A. B. Phillips, B. L. Tompkins, R. J. Ellingson and M. J. Heben, *Chem. Mater.*, 2015, **27**, 4612.
2. O. Flender, J. R. Klein, T. Lenzer and K. Oum, *Phys. Chem. Chem. Phys.*, 2015, **17**, 19238.
3. J. S. Manser and P. V. Kamat, *Nat. Photonics*, 2014, **6**, 737.
4. I. Robel, B. A. Bunker, P. V. Kamat and M. Kuno, *Nano Lett.*, 2006, **6**, 1344.